Shearflow effects on selfassembly of semidilute solutions of offcritical polymer mixtures: Shearhysteresis effects

Koji Asakawa and Takeji Hashimoto

Citation: The Journal of Chemical Physics **105**, 5216 (1996); doi: 10.1063/1.472364
View online: http://dx.doi.org/10.1063/1.472364
View Table of Contents: http://scitation.aip.org/content/aip/journal/jcp/105/12?ver=pdfcov
Published by the AIP Publishing

Shear-flow effects on self-assembly of semidilute solutions of off-critical polymer mixtures: Shear-hysteresis effects

Koji Asakawa[a] and Takeji Hashimoto
Department of Polymer Chemistry, Graduate School of Engineering, Kyoto University, Kyoto 606-01, Japan

(Received 27 October 1995; accepted 20 June 1996)

We use flow light scattering to study the phase transitions in semidilute solutions of polystyrene and polybutadiene in dioctylphthalate under simple shear flow. The phase-separated solution was brought into a single-phase state by increasing the shear rate, $\dot{\gamma}$, above a critical shear rate, $\dot{\gamma}_{c,i}$. The solution was then brought back into a two-phase state by lowering $\dot{\gamma}$ below a critical shear rate, $\dot{\gamma}_{c,d}$. We previously reported a large hysteresis effect in solutions with off-critical compositions; $\dot{\gamma}_{c,i}$ is always higher than $\dot{\gamma}_{c,d}$. Shear-drop experiments were conducted to illuminate the origin of this hysteresis effect. The experimental results showed that at temperatures close to the cloud point temperature the formation of phase separated structures did not occur until up to 22 h after lowering the shear rate below $\dot{\gamma}_{c,i}$. Thus the hysteresis effect was found to be due to a surprisingly slow ordering process at $\dot{\gamma}$ close to $\dot{\gamma}_{c,i}$. The ordering induced by the shear drop needs a much longer time than the homogenization induced by increasing shear. If the time scale of observation is sufficiently long, the hysteresis effect disappears, yielding the drop of cloud point temperature with shear, $\Delta T_c(\dot{\gamma})$, given by $\Delta T_c(\dot{\gamma}) \propto \dot{\gamma}^{1.0\pm0.1}$ for the off-critical mixtures, rather than $\Delta T_c(\dot{\gamma}) \propto \dot{\gamma}^{0.5\pm0.1}$ found previously for the near critical mixtures. Finally, the incubation time was found to initially increase with $\dot{\gamma}$ and then decrease with a further increase of $\dot{\gamma}$, suggesting that the ordering mechanisms are different in the low and high shear-rate regimes. © *1996 American Institute of Physics.* [S0021-9606(96)51136-0]

I. INTRODUCTION

The effects of shear flow on the phase transitions and self-assembly (i.e., phase-separated structures and phase-separation kinetics, mechanisms and processes) of multicomponent mixtures have not yet been fully investigated, though an exploration of them is an intriguing subject in statistical physics.[1–17] The flow light-scattering method[18] has been used to investigate shear effects in a ternary system consisting of polystyrene(PS), polybutadiene(PB), and dioctylphthalate(DOP) in previous reports.[8–10,13,19,20] DOP was chosen as an approximately neutral solvent to PS and PB. Therefore, it should be equally partitioned between the two phases when phase separation occurs between the polymers, giving the system a pseudobinary character.[21] This solvent reduces effective repulsive interactions between PS and PB and hence can bring the coexistence curve of the system to an easily accessible temperature range.

In previous studies,[8–10,13,19,20] we have presented the ordered structures and the shear-induced homogenization (single-phase formation) of semidilute solutions of polymer mixtures under simple shear flow. We observed the large hysteresis effect shown in Fig. 1 for the off-critical mixtures, though not for near-critical mixtures.[19] For the off-critical mixtures, the change in the scattered intensity with the increasing shear rate is very different from that with the decreasing shear rate; and the critical shear rate, $\dot{\gamma}_{c,i}$, for the phase transition from the two-phase state to the single-phase state in increasing shear rate cycles is much higher than the critical shear rate, $\dot{\gamma}_{c,d}$, for the transition from the single-phase state to the two-phase state in decreasing shear-rate cycles.

In this paper, we focus on this shear-hysteresis effect in the off-critical mixtures and investigate experimentally the origin of this effect and physical factors controlling this effect by means of the flow-light scattering method.[18] For this purpose, rather than employing a shear-rate sweeping method, we employed a shear-drop method in which we quickly lower the shear rate, $\dot{\gamma}$, from a shear rate higher than $\dot{\gamma}_{c,i}$ (the solutions being in the shear-induced single-phase state) to a shear rate lower than $\dot{\gamma}_{c,i}$ (the solutions being in the two-phase state) and observe the isothermal ordering phenomena in the solutions. We aim to report pieces of evidence that we found in these shear-drop experiments.

II. EXPERIMENTAL METHODS

A. Materials

We used various blends of PS and PB dissolved in DOP for this study. The PS has a weight average molecular weight (Mw) and a number average molecular weight (Mn) of 2.14×10^5 and 2.04×10^5, respectively. The PB has a Mw of 3.13×10^5 and a Mn of 1.65×10^5. The PS and PB were mixed in the ratios of 80/20, 50/50, and 20/80 (wt/wt). Solutions were prepared by dissolving a prescribed amount of PS, PB, and DOP in an excess of methylene chloride and evaporating the methylene chloride completely. The resulting solutions had a composition of 3.3 wt. % polymer in DOP. The total polymer concentration, c, satisfies the condition $c \approx 2c^*$, where c^* is the overlap concentration of the

[a]Present address: Toshiba Research and Development Center, 1 Komukai Toshiba-cho, Saiwai-ku, Kawasaki 210, Japan.

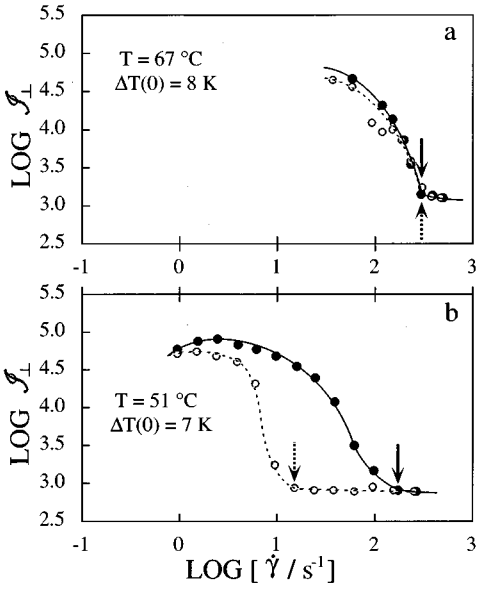

FIG. 1. Shear rate dependence of the integrated intensity, $\mathscr{I}_\perp$, for the PS/PB mixtures of (a) 50/50 at $\Delta T(0)=8$ K and (b) 80/20 at $\Delta T(0)=7$ K. The solid lines show the results obtained in the increasing shear-rate cycles and the broken lines show those in the decreasing cycles.

polymer coils.[22] Thus, solutions used in this study were semidilute and the polymer coils were weakly overlapped and entangled.

B. Flow small-angle light scattering

The flow small-angle light scattering apparatus and techniques were described elsewhere.[10,18] A coordinate system, O_{xyz}, was set with the axes O_x and O_z taken parallel to the propagation direction of the incident light beam and to the shear flow direction, respectively, as in our previous paper.[10,18] Thus, the velocity gradient exists along the axis, O_x, in the plane, O_{xz}. In order to investigate the structures occurring under shear-flow, we measured the *in situ* light scattering intensity, $I(q_y,q_z)$, as a function of the scattering vector, **q**, on the detector plane, O_{yz}, by using a photodiode array detector.[10] The vector, **q**, on the detector plane consists of the y and z components, q_y and q_z, respectively, but the x component, q_x, is equal to zero. Thus the intensity is described as a function of q_y and q_z, i.e., $I(q_y,q_z)$. The magnitude, q, of the scattering vector is related to the wavelength, λ, of the incident beam and the scattering angle, θ, in the solution by

$$q=(4\pi/\lambda)\sin(\theta/2). \tag{1}$$

In order to determine the cloud point temperature, $T_c(\dot{\gamma})$, at a given shear rate, $\dot{\gamma}$, or the critical shear rate, $\dot{\gamma}_c(T)$, for the single-phase formation at a given T, the integrated intensity normal to the flow direction, $\mathscr{I}_\perp$, was measured as a function of $\dot{\gamma}$ at various temperatures with a linear photodiode array placed on the detector plane normal to the flow direction. The intensity $\mathscr{I}_\perp$ was defined by

$$\mathscr{I}_\perp \equiv \int_{-q_z''}^{q_z''} dq_z \int_{q_y'}^{q_y''} dq_y I(q_y,q_z). \tag{2}$$

The values q_y'' and q_y' are, respectively, the upper and lower bounds of q_y ($q_y''=1.8\times10^{-3}$ nm^{-1} and $q_y'=6.6\times10^{-4}$ nm^{-1}) covered by the linear array and q_z'' is the magnitude of the scattering vector subtended by the height limiting slit placed in front of the photodiode array ($q_z''=3.7\times10^{-5}$ nm^{-1}). We will discuss results in terms of quench depth, $\Delta T(0)$, as defined by

$$\Delta T(0)\equiv T_c(0)-T, \tag{3}$$

where $T_c(0)$ is the cloud point temperature at zero shear (quiescent state) [$T_c(\dot{\gamma})$ at $\dot{\gamma}=0$] and T is the temperature at which the experiment was performed.

III. RESULTS AND DISCUSSION

A. Hysteresis effects

Figure 1 shows typical examples of the $\dot{\gamma}$-dependence of the integrated intensity, $\mathscr{I}_\perp$, for (a) PS/PB mixtures of 50/50 (wt/wt) at $\Delta T(0)=8$ K and (b) 80/20 (wt/wt) at $\Delta T(0)=7$ K. Hereafter we suppress (wt/wt) in describing compositions of the mixtures for simplicity. The solid and broken lines show the results obtained in the increasing and decreasing shear-rate cycles, respectively. In these experiments the shear rate was changed stepwise in both the increasing and decreasing shear-rate cycles, and $\mathscr{I}_\perp$ at a given $\dot{\gamma}$ was measured 20 min after imposing a given shear rate on the solution. For the 50/50 mixture, which is close to the near-critical composition, the hysteresis effects appear to be weak or nonexistent, since the $\mathscr{I}_\perp$ at various $\dot{\gamma}$ agree well for the increasing and decreasing cycles of shear rate. For the 80/20 mixture, however, which is an off-critical composition, a large hysteresis effect was observed with the limited observation time of 20 min. The critical shear rates for the homogenization in the increasing cycles, $\dot{\gamma}_{c,i}$, shown by the solid arrow were always found to be higher than the phase separation shear rates in the decreasing cycles, $\dot{\gamma}_{c,d}$, shown by the broken arrow. The greater hysteresis effects, $\delta\dot{\gamma}_c\equiv\dot{\gamma}_{c,i}-\dot{\gamma}_{c,d}$, were found at lower quench depths, $\Delta T(0)$, for the off-critical mixture; the hysteresis effects diminish with increasing the quench depth as demonstrated previously.[19] These hysteresis effects led to the following empirical expressions for the cloud-point temperature drop with $\dot{\gamma}$ for the off-critical mixtures[19]

$$\Delta T_c(\dot{\gamma})/T_c(0) \propto \begin{cases} \dot{\gamma}^{0.5\pm0.1} & \text{for decreasing cycles of } \dot{\gamma} \quad (4a) \\ \dot{\gamma}^{1.0\pm0.1} & \text{for increasing cycles of } \dot{\gamma} \quad (4b) \end{cases}.$$

Note that the cloud-point temperature drop for the *near-critical mixture* was expressed[19] by Eq. (4a) for *both decreasing and increasing cycles of* $\dot{\gamma}$.

In this work we would like to investigate whether or not the hysteresis effects summarized in Eqs. (4a) and (4b) are a phenomenon which depends on time scale of observations. If

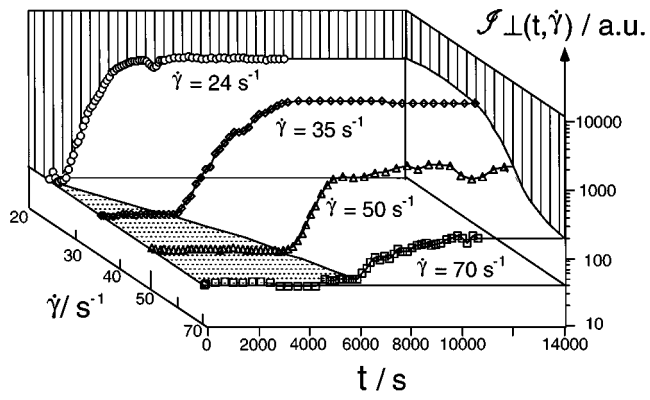

FIG. 2. Three-dimensional representation of the results of the shear-drop experiments of the PS/PB (80/20) mixtures at a quench depth, $\Delta T(0)$, of 10 K. The shear rate, $\dot\gamma$, to produce a homogeneous state before the shear drop was greater than $\dot\gamma_{c,i}$ ($=160$ s^{-1}).

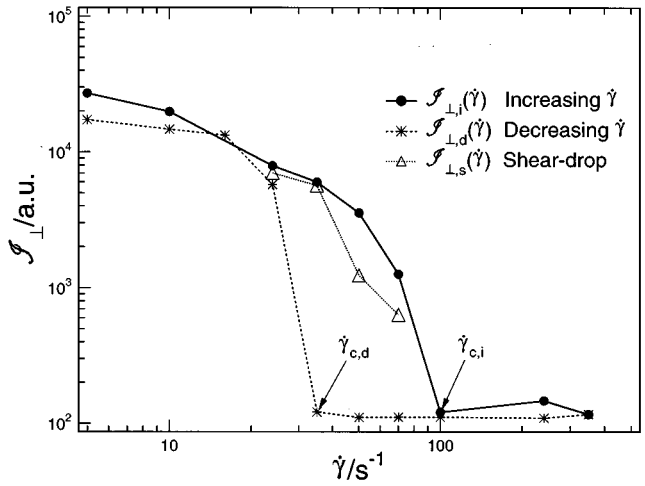

FIG. 3. Comparison of the $\dot\gamma$-dependence of $\mathscr{I}_\perp$ obtained from the increasing ($\mathscr{I}_{\perp,i}$, $-\cdot-$) and decreasing cycles of $\dot\gamma$ ($\mathscr{I}_{\perp,d}$, ---*---) with that of the intensity at steady state obtained by the shear-drop experiments $\mathscr{I}_{\perp,s}$ ($-\Delta-$) for the PS/PB (80/20) mixture at a quench depth, $\Delta T(0)$, of 10 K. The lines connecting data points are drawn for visual guides.

so, what kind of an expression can we obtain for $\Delta T_c(\dot\gamma)/T_c(0)$ vs $\dot\gamma$ with a sufficiently long time scale of observations? Moreover, in the long time-limit are the expressions the same for the critical and off-critical mixtures?

B. Shear-drop experiment

It would be useful to investigate the ordering of the structures as a function of time under isothermal conditions, i.e., at a given set of $\Delta T(0)$ and $\dot\gamma$, in order to gain insight into the reason for the hysteresis effects. For this purpose, *shear-drop experiments* were conducted for the off-critical mixtures. The system at the given $\Delta T(0)$ was first brought into a single-phase state by applying a shear flow of $\dot\gamma > \dot\gamma_{c,i}$.[8–10] After the system became completely homogeneous, $\dot\gamma$ was then suddenly dropped to a certain constant value $\dot\gamma$ below $\dot\gamma_{c,i}$ and the resulting phase separation process was investigated as a function of time.

Figure 2 shows the results of the shear-drop experiments for the 80/20 mixtures at a quench depth, $\Delta T(0)$, of 10 K. The system was first brought into a single-phase state by shearing at $\dot\gamma$ which is greater than $\dot\gamma_{c,i}$ (160 s^{-1}) and then the shear rate was dropped to various $\dot\gamma$ values (24, 35, 50, 70 s^{-1}) below the $\dot\gamma_{c,i}$ value as shown in the figure. Finally, the time evolution of the integrated intensity normal to flow, $\mathscr{I}_\perp$, at each shear rate, $\dot\gamma$, was observed. We found that the ordering process (or the change in $\mathscr{I}_\perp$) after the shear drop hardly depended on the shear rate imposed on the system for the formation of the single-phase-state; any shear rates higher than $\dot\gamma_{c,i}$ gave the same results. At a given shear rate below $\dot\gamma_{c,i}$, $\mathscr{I}_\perp$ generally stayed at the same level as for the homogeneous state for a while. Then, after a certain incubation time, $t_{\rm inc}(\dot\gamma)$, which depends on $\dot\gamma$, $\mathscr{I}_\perp$ increased and eventually reached a shear-rate-dependent *steady value*, $\mathscr{I}_{\perp,s}$. This $t_{\rm inc}(\dot\gamma)$ was found to increase with increasing $\dot\gamma$. The time interval between $t_{\rm inc}(\dot\gamma)$ and the time at which the steady value of $\mathscr{I}_{\perp,s}$ was attained also appeared to increase with $\dot\gamma$, ~3000, 4000, 4000, and 5000 s at $\dot\gamma = 24$, 35, 50, and 70 s^{-1}, respectively. Thus the time required for achieving $\mathscr{I}_{\perp,s}$ strongly depends on $\dot\gamma$ and can be very long as $\dot\gamma$ approaches $\dot\gamma_{c,i}$, e.g., ~11 000 s (3 h) at $\dot\gamma = 70$ s^{-1}. The *steady values*, $\mathscr{I}_{\perp,s}$, were found to decrease with $\dot\gamma$, which reflects the changes in the steady structures as a function of $\dot\gamma$ as elucidated in our earlier work.[9,13] Moreover, $\mathscr{I}_{\perp,s}(\dot\gamma)$ was found to be in good agreement with $\mathscr{I}_{\perp,i}(\dot\gamma)$ obtained from the increasing cycles of $\dot\gamma$, as will be more clearly indicated in Fig. 3 below.

The results shown in Fig. 2 clarified the following points concerning the phase-separation processes for the off-critical mixture: (i) The phase-separated structure, as observed by light scattering, is formed after a certain incubation time, $t_{\rm inc}(\dot\gamma)$, which depends on shear rate, $\dot\gamma$, and at $t < t_{\rm inc}$, the system remains homogeneous in the length scale covered in this experiment; (ii) After the incubation period, the structure formation starts to occur and eventually steady state structures are formed. The time required for this ordering process increases with $\dot\gamma$ under the conditions of this experiment.

Figure 3 compares the shear-rate dependence of the integrated intensity normal to flow for the increasing and decreasing cycles of $\dot\gamma$ as well as that of the steady values of $\mathscr{I}_\perp$ obtained from the shear-drop experiments. We denote the resulting quantities as $\mathscr{I}_{\perp,i}$, $\mathscr{I}_{\perp,d}$, and $\mathscr{I}_{\perp,s}$, respectively. The data for $\mathscr{I}_{\perp,s}$ were closer to those of $\mathscr{I}_{\perp,i}$ obtained from the increasing shear-rate cycles than those for $\mathscr{I}_{\perp,d}$ of the decreasing cycles. This means that the integrated intensity for the decreasing shear-rate cycle, $\mathscr{I}_{\perp,d}$, approaches that of the steady values of $\mathscr{I}_{\perp,s}$ for the shear-drop experiments, if the time scale of the observation at each shear rate is sufficiently long. This means if we wait long enough $\mathscr{I}_{\perp,i}$ and $\mathscr{I}_{\perp,d}$ will be equal, so that the hysteresis is an artifact of the measuring time.

Thus the hysteresis effects are shown to result from the slow ordering processes of the domain structures from the shear-homogenized solution when $\dot\gamma$ is lowered below $\dot\gamma_{c,i}$ (not $\dot\gamma_{c,d}$). The effects are clearly shown to depend on the time scale of the observation; $\delta\dot\gamma_c$ tends to diminish if the

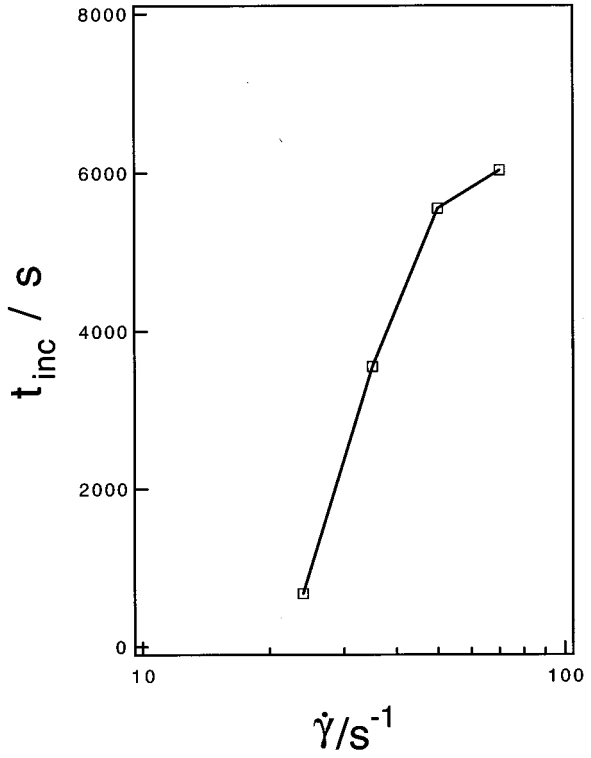

FIG. 4. Shear-rate dependence of the incubation time ($t_{\rm inc}$) obtained from the shear-drop experiments shown in Fig. 2.

time scale of the observation is long enough (longer than ~12 000 s as clearly illuminated from the result at $\dot{\gamma}=70\ s^{-1}$ shown in Fig. 2). The small discrepancies between $\mathscr{I}_{\perp,i}$ and $\mathscr{I}_{\perp,s}$ in Fig. 3 may arise from a finite time scale employed in the experiments of the increasing shear-rate cycle. If the time scale of the observation for the increasing cycle is made longer, the values $\mathscr{I}_{\perp,i}$ will drop to the levels of $\mathscr{I}_{\perp,s}$.

Figure 4 shows that the incubation time for the ordering process tends to increase with increasing $\dot{\gamma}$. Accordingly, the time required to attain a steady state value of $\mathscr{I}_{\perp,s}$ becomes longer with increasing $\dot{\gamma}$.

Figure 5 shows another example on the time-evolution of $\mathscr{I}_\perp$ at various $\dot{\gamma}$ after the shear drop from 847 s^{-1} for the same solution as in Fig. 2 but at a larger $\Delta T(0)$ (14 K). The homogenization shear rate of the increasing cycle, $\dot{\gamma}_{c,i}$, was 593 s^{-1} at this $\Delta T(0)$. At a given $\dot{\gamma}<\dot{\gamma}_{c,i}$, $\mathscr{I}_\perp$ started increasing after a certain incubation time and reached a steady value after a time, as in the experiments shown in Fig. 2. The value of $\mathscr{I}_\perp$ during the incubation time was the same as that of the homogeneous state at a shear rate of 847 s^{-1}. The steady state value of $\mathscr{I}_{\perp,s}(\dot{\gamma})$ obtained after the shear drop also agreed well with $\mathscr{I}_{\perp,i}(\dot{\gamma})$ obtained from the increasing shear-rate cycles. The same tendencies were observed for all $\dot{\gamma}$. All of the trends described above are the same as those at $\Delta T(0)=10$ K (Fig. 2) except for the incubation time. It is quite striking to note that the incubation time increases with increasing $\dot{\gamma}$ in a low shear-rate regime ($\dot{\gamma}\lesssim 110\ s^{-1}$) but decreases with a further increase of $\dot{\gamma}$ in a high shear-rate regime ($\dot{\gamma}>110\ s^{-1}$).

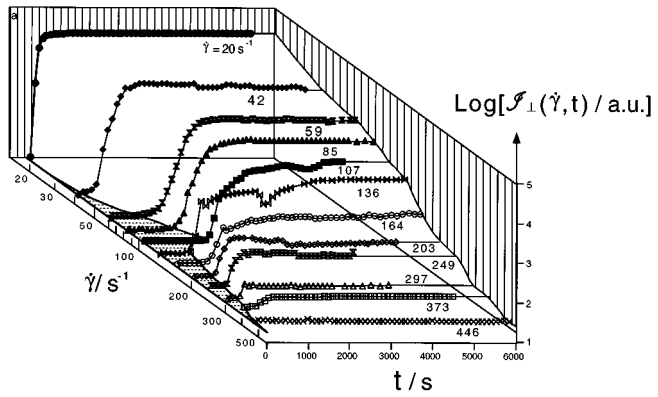

FIG. 5. Time-evolution of $\mathscr{I}_\perp$ for the off-critical mixture (PS:PB=80:20) at various $\dot{\gamma}$ at a $\Delta T(0)$ of 14 K after the shear drop from 847 s^{-1}. $\dot{\gamma}_{c,i}$ was 593 s^{-1}.

The time evolution of $\mathscr{I}_\perp$ after the shear drop in the low shear regime is shown in Fig. 6(a). We note the following: (i) No incubation time was observed at a shear rate of 20 s^{-1}, but increasing incubation time with increasing $\dot{\gamma}$ is observed; (ii) The increase of $\mathscr{I}_\perp$ to the steady value of $\mathscr{I}_{\perp,s}(\dot{\gamma})$ becomes slower with increasing $\dot{\gamma}$. These tendencies were the same for the shear-drop experiments at $\Delta T(0)=10$ K shown in Fig. 2.

As shown in Fig. 6(b), in the high $\dot{\gamma}$ regime ($\dot{\gamma}>110\ s^{-1}$), however, the incubation time decreased with increasing $\dot{\gamma}$. It did not take a long time for $\mathscr{I}_\perp$ to reach a constant level of $\mathscr{I}_{\perp,s}(\dot{\gamma})$ which was approximately the same intensity as $\mathscr{I}_{\perp,i}(\dot{\gamma})$ obtained from the increasing shear-rate cycles, al-

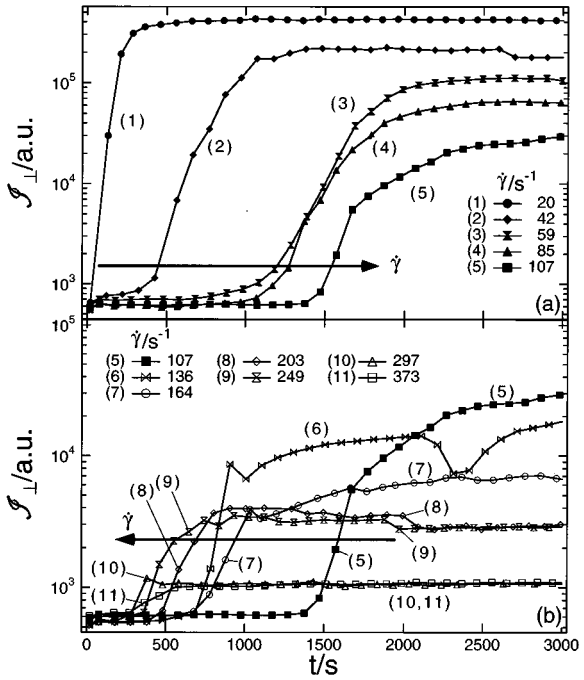

FIG. 6. Time-evolution of $\mathscr{I}_\perp$ after the shear drop to the various values of $\dot{\gamma}$ in the same experiments as in Fig. 5.

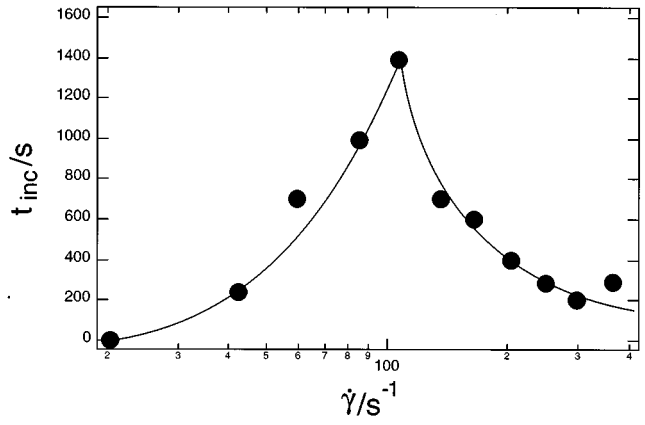

FIG. 7. Variation of $t_{\rm inc}(\dot\gamma)$ against $\dot\gamma$ in the same experiment as in Fig. 5.

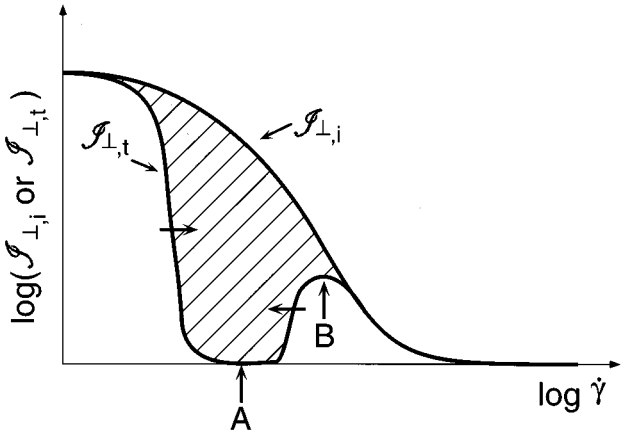

FIG. 9. Schematic diagram showing $\mathscr{I}_{\perp,i}$ and $\mathscr{I}_{\perp,t}$ as a function of $\dot\gamma$. As the time scale of observation (i.e., the time spent after the shear drop) increases the shaded area narrows as indicated by the arrows, and $\mathscr{I}_{\perp,t}$ approaches $\mathscr{I}_{\perp,i}$.

though the scattering intensities were very weak in this high shear-rate regime.

The variation of $t_{\rm inc}(\dot\gamma)$ against $\dot\gamma$ is summarized in Fig. 7. It shows that the incubation time increased from 0 s at a shear rate of 20 s^{-1} to 1400 s at a shear rate of 107 s^{-1} but it decreased upon further increasing the shear rate. The variation of $t_{\rm inc}(\dot\gamma)$ with $\dot\gamma$ suggests that different mechanisms of the phase separation and ordering occur in the low and high shear-rate regimes after the shear drop from a single phase state.

Figure 8 shows the integrated intensities, $\mathscr{I}_{\perp,t}$, at various fixed times after the shear drop. Each curve in the figure was constructed from the results shown in either Fig. 5 or Fig. 6 as follows. The intensity, $\mathscr{I}_{\perp,t}$, at a certain time, t, after the shear drop was evaluated at each $\dot\gamma$, and the isochronal intensity data thus obtained at $t=0$, 500, 1500, 2000, and 6000 s were plotted as a function of $\dot\gamma$. The thin solid lines numbered (1)–(4) are visual guides for the data of $\mathscr{I}_{\perp,t}$ at $t=0$, 500, 1500, and 2000 s, respectively. Figure 8 includes the shear-rate dependence of the intensity, $\mathscr{I}_{\perp,i}$, obtained in the increasing shear-rate cycle (data shown by the thick solid line) for comparison.

Figure 8 should be useful to demonstrate how the shear-rate dependence of $\mathscr{I}_{\perp,d}$ depends on the time scale of observation. If the time, t, after the shear drop is extremely short, $\mathscr{I}_{\perp,t}(\dot\gamma)$ has an intensity level identical to that of the single-phase state [see curve (1) at $t=0$ in Fig. 8]; the system appears as if it were in single-phase state even at $\dot\gamma \ll \dot\gamma_{c,i}$. $\mathscr{I}_{\perp,t}(\dot\gamma)$ obtained at moderate times after the shear drop has the $\dot\gamma$-dependence schematically shown in Fig. 9; $\mathscr{I}_{\perp,t}$ agrees with $\mathscr{I}_{\perp,i}$ at low shear rates but it becomes much less than $\mathscr{I}_{\perp,i}$ with increasing $\dot\gamma$ and reaches a minimum intensity (point A), the level of which is identical to the intensity from the homogeneous solutions; upon further increasing $\dot\gamma$, however, $\mathscr{I}_{\perp,t}$ increases again to a maximum (at point B) and becomes equal to $\mathscr{I}_{\perp,i}$; with a further increase of $\dot\gamma$, both $\mathscr{I}_{\perp,t}$ and $\mathscr{I}_{\perp,i}$ eventually decrease to the intensity level for the homogenized solution.[23] This trend is actually found as

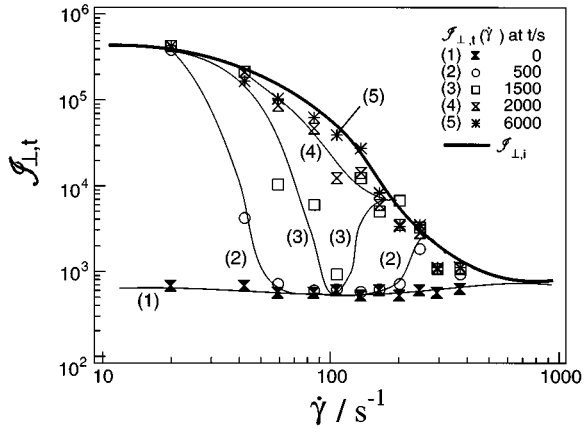

FIG. 8. Integrated intensity $\mathscr{I}_{\perp,t}(\dot\gamma)$ obtained at fixed times after the shear drop. Curves (1)–(5) correspond, respectively, to $\mathscr{I}_{\perp,t}$ at $t=0$, 500, 1500, 2000, and 6000 s. The thick solid line shows the integrated intensity $\mathscr{I}_{\perp,i}$ obtained from the shear-rate sweep experiments during the increasing shear-rate cycles.

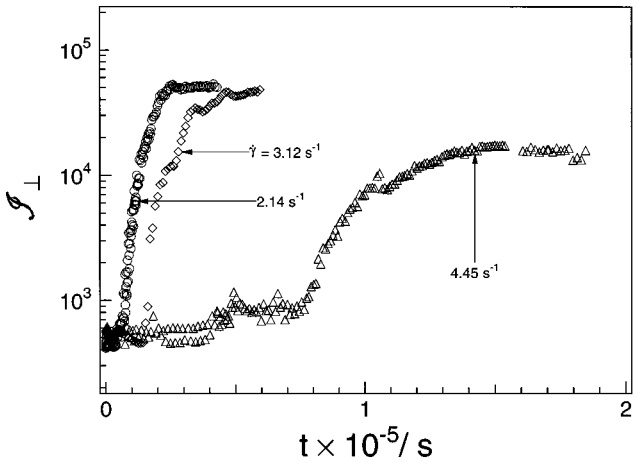

FIG. 10. Extreme examples of the slow phase-separation process as observed from the time-evolution of $\mathscr{I}_{\perp}$ after the shear-drop from $\dot\gamma > \dot\gamma_{c,i}$ to the various values of $\dot\gamma(<\dot\gamma_c)$ for the solution with $\Delta T(0)=4$ K.

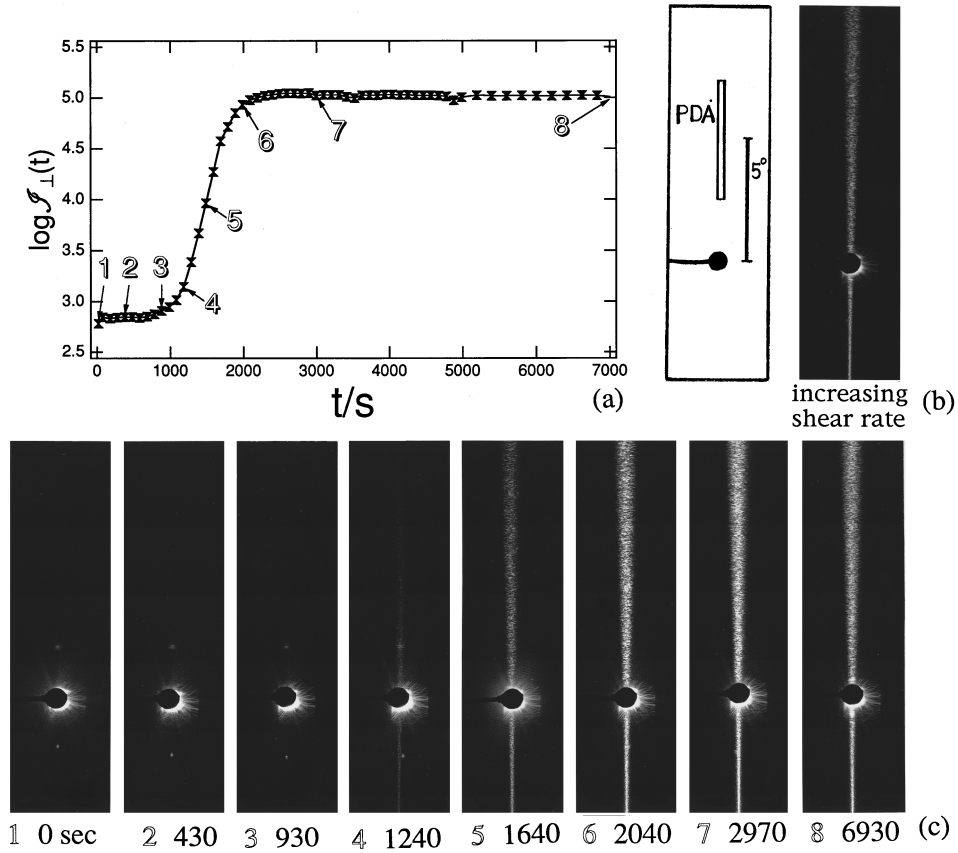

FIG. 11. Time variation of the scattering pattern after the shear drop to $\dot{\gamma}=59\ \mathrm{s}^{-1}$ at $\Delta T(0)=14$ K (the low shear regime identified by Figs. 5 or 7). (a) The time-evolution of the integrated scattered intensity, $\mathscr{I}_\perp(t)$, normal to flow. The integrated intensity shown in (a) was obtained over the area marked by the PDA in part (b) and the bar for 5° denotes the scattering angle in the solution. (b) The scattering pattern taken at $\dot{\gamma}=59\ \mathrm{s}^{-1}$ during the increasing shear-rate cycle. (c) The time variation of the scattering pattern after the shear drop. The numbers 1–8 in part (c) correspond to those in part (a), indicating the integrated intensity, $\mathscr{I}_\perp$, for each scattering pattern.

shown in Fig. 8. The discrepancy of $\mathscr{I}_{\perp,i}$ and $\mathscr{I}_{\perp,t}$ (a hysteresis effect) decreases, i.e., the shaded area shown in Fig. 9 narrows and point A moves upward with increasing the time spent after the shear drop, i.e., the time scale of our observation.

It should be noted in Fig. 8 that the $\mathscr{I}_{\perp,t}$ values at $t=6000$ s are almost identical to the steady values of $\mathscr{I}_{\perp,t}$ obtained after the shear drop. Since $\mathscr{I}_{\perp,i}$ and $\mathscr{I}_{\perp,s}$ agree well, the hysteresis observed at $\Delta T(0)=14$ K is not considered to be an intrinsic hysteresis but simply due to a time-dependent phenomenon, i.e., a slow ordering process after the shear-drop below $\dot{\gamma}_{c,i}$. These data also show that the phase-separation process needs a much longer time than the homogenization process under shear flow.

The results obtained from the shear-drop experiments (see Figs. 3 and 8) showed that the steady values of $\mathscr{I}_{\perp,s}$ obtained after the shear-drop are nearly equal to the values of $\mathscr{I}_{\perp,i}$ for the increasing shear-rate cycles. This means that in the long time limit the behavior of the solution obtained during the cycle of decreasing shear rate is the same as that obtained during the cycle of increasing shear rate. This conclusion further produces the following result: the relation given by Eq. (4a) previously found for decreasing cycles of $\dot{\gamma}$ should be modified to the form

$$\Delta T_c(\dot{\gamma})/T_c(0)\propto\dot{\gamma}^{1.0\pm0.1}, \tag{5}$$

when the steady state is truly established. This result becomes identical to Eq. (4b) obtained for increasing cycles of $\dot{\gamma}$. Thus we can conclude that the cloud-point temperature drop with shear flow for the off-critical mixture is definitely different from that for the critical mixture (which has the exponent of $\dot{\gamma}$ equal to 0.5 ± 0.1,[10] for both increasing and decreasing cycles of shear rate).[24]

It was found that the phase separation processes after the shear drop need much longer times than we thought compared to the homogenization processes under the shear flow. Figure 10 shows an extreme example of the slow phase separation process as observed from the time-evolution of $\mathscr{I}_\perp(\dot{\gamma})$ after the shear drop from $\dot{\gamma}>\dot{\gamma}_{c,i}$ (homogeneous) to $\dot{\gamma}<\dot{\gamma}_{c,i}$ (phase separated) for the same solution but at a different quench depth of $\Delta T(0)=4$ K. Note that $\Delta T(0)$ was 10 K and 14 K in the cases of Figs. 2 and 5 (or 6), respectively. The sample was first homogenized at a shear rate of $85\ \mathrm{s}^{-1}$ (Fig. 10). The incubation time generally increases with increasing $\dot{\gamma}$ in the shear-rate range covered by the experiment.[25] The incubation time was found to be as long as 7.5×10^4 s (21 h) in the case of $\dot{\gamma}$ equal to $4.45\ \mathrm{s}^{-1}$. To reach steady state, it took more than 1.5×10^5 s (41 h, 2 days).

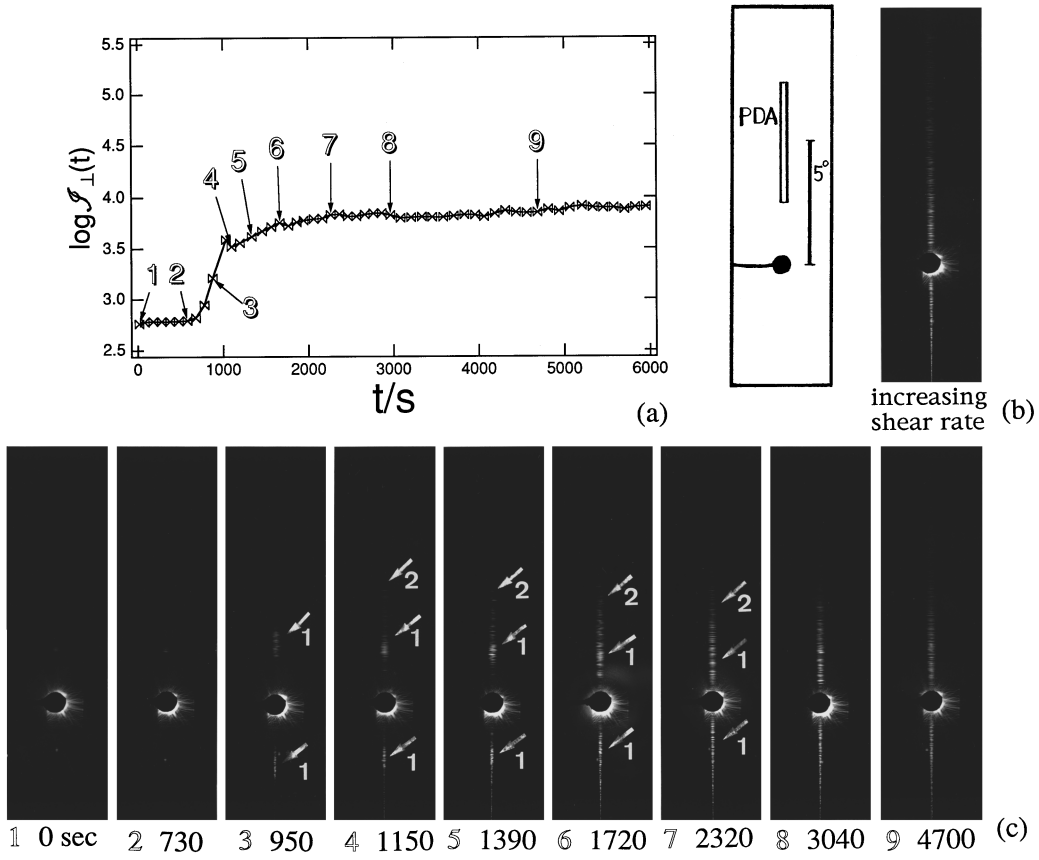

FIG. 12. Time variation of the scattering pattern after the shear drop to $\dot{\gamma}=136\ \mathrm{s}^{-1}$ at $\Delta T(0)=14$ K (the high shear regime identified by Figs. 5 or 7). (a) The time-evolution of the integrated intensity, $\mathscr{I}_\perp$. The integrated intensity shown in (a) was obtained over the area marked by the PDA in part (b) and the bar for 5° denotes the scattering angle in the solution. (b) The scattering pattern taken at $\dot{\gamma}=136\ \mathrm{s}^{-1}$ during the increasing shear-rate cycle. (c) The time variation of the scattering pattern after the shear drop. The numbers 1–9 in part (c) correspond to those in part (a), indicating the integrated intensity, $\mathscr{I}_\perp$, for each scattering pattern.

Thus, the time interval of the decreasing shear cycles would need at least 41 h, otherwise the scattering intensity of the true steady state cannot be observed.

The time-evolution of $\mathscr{I}_\perp(\dot{\gamma})$ after the shear drop for the solution at $\Delta T(0)=14$ K (Figs. 5–7) suggests that the transient structures that appear during the phase separation in the low shear-rate ($\dot{\gamma}\lesssim 110\ \mathrm{s}^{-1}$) and high shear-rate regimes ($\dot{\gamma}>110\ \mathrm{s}^{-1}$) may be quite different, i.e., the ordering mechanism in the phase separation may be different above and below a certain shear rate. In order to investigate this point, it is useful to study the time-evolution of the scattering intensity distributions themselves during the phase separation.

The time variation of the scattering pattern after the shear drop at $\Delta T(0)=14$ K and $\dot{\gamma}=59\ \mathrm{s}^{-1}$ shown in Fig. 11 is representative of the behavior at the lower shear regime. The flow direction (z-axis) was taken along the horizontal direction and the neutral (y) axis in the vertical direction in the patterns shown in parts (b) and (c). The pattern in part (b) shows the scattering pattern taken during the increasing shear-rate cycle. The integrated intensity shown in part (a) was obtained over the area as shown in the photodiode array (PDA) in the schematic diagram shown in part (b) and the angle of 5° denotes the scattering angle in the solution. A streaklike scattering elongated perpendicular to the flow was observed from the beginning of the appearance of the scattering pattern. It suggests that the domain structures developed after a certain incubation time in the phase separation induced by the shear drop are highly elongated and oriented along the flow direction. The scattering intensity increased simultaneously at all q and the scattering intensity distribution with respect to q did not change with time from the beginning to the end of the phase separation process, over the time scale and q scale covered in our experiments. This suggests that the elongated domains do not change in shape but only the number of domains increases and/or the contrast of the two phases increases.

The steady-state scattering pattern [e.g., the pattern at 6930 s in part (c)] obtained after the shear drop is essentially identical to that obtained in the increasing shear-rate cycles [the pattern in part (b)]. These scattering profiles suggest the formation of a ''string phase'' in the steady state, e.g., an assembly of the highly elongated cylinders along the flow.[26] It is clearly necessary to investigate the possible ordering processes occurring outside the q-window of our observation during the incubation time. Investigation along this line is now in progress in our laboratory.

On the other hand, the scattering pattern after the shear

drop in the high shear regime was considerably different from that in the low shear regime. The time variation of the scattering pattern after the shear drop at $\Delta T(0)=14$ K and $\dot{\gamma}=136\ s^{-1}$ shown in Fig. 12 is representative of the high shear regime. Again sharp streaklike patterns appear normal to the flow direction. However, it is quite striking to note that in this case a scattering maximum was observed along the direction perpendicular to the flow during the course of the phase separation. It then moves to the smaller angle and its intensity increases with time. After a while, second and even third-order peaks were observed outside the first-order peak and move to smaller angles like the first-order peak. Finally, the peaks disappeared or moved to the angles inside the beam stop and the pattern shows the streaklike pattern identical to that obtained in the increasing shear-rate cycles. We note that the high-order peaks appeared at the positions of approximately $\sqrt{3}$ and $\sqrt{4}$ relative to the first order peak position, possibly suggesting that concentration fluctuations with hexagonal symmetry normal to flow grow with time.

IV. CONCLUSION

The shear-drop experiments revealed that the hysteresis effect observed for off-critical mixtures is due to a slow ordering process of the homogeneous solution when $\dot{\gamma}$ is dropped below $\dot{\gamma}_{c,i}$. At a small quench depth $\Delta T(0)$, the ordering takes a surprisingly long time, up to ~40 h. This ordering process needs a much longer time than the homogenization process induced by increasing $\dot{\gamma}$. Thus the structure formation during the decreasing cycle of $\dot{\gamma}$ requires more time than the structure dissolution during the increasing cycle. At a long time scale of observation, the hysteresis effect disappears, yielding Eq. (5) for the drop of the reduced cloud point temperature with $\dot{\gamma}$ for off-critical mixtures both for the increasing and decreasing cycles of $\dot{\gamma}$. Thus it turns out that the off-critical mixtures show definitely different behavior from the critical mixture in the shear-rate dependence of the cloud point.

The structure formation from the homogeneous solution, induced by the shear-drop and as observed by the light scattering method, was found to occur after a certain incubation time $t_{\rm inc}\ [\dot{\gamma},\Delta T(0)]$ which depends on $\dot{\gamma}$ and the quench depth, $\Delta T(0)$. At a given $\Delta T(0)$, $t_{\rm inc}$ tends to increase with $\dot{\gamma}$ and then decreases with a further increase of $\dot{\gamma}$. The ordering mechanisms are inferred to be quite different above and below this turning shear rate. However a further study of this phenomenon is left for future work.

ACKNOWLEDGMENTS

The authors thank A. Onuki for valuable discussion. This work was supported in part by a Grant-in-Aid for Scientific Research on Priority Areas, ''Cooperative Phenomena in Complex Liquids,'' Ministry of Education, Science, Sports, and Culture, Japan (07236103).

[1] A. Silberberg and W. Kuhn, J. Polym. Sci. **13**, 21 (1954).
[2] G. Ver Strate and W. Phillippoff, J. Polym. Sci. Polym. Lett. Ed. **12**, 267 (1974).
[3] R. Schmidt and B. A. Wolf, Colloid. Polym. Sci. **257**, 1187 (1979).
[4] A. Onuki and K. Kawasaki, Ann. Phys. (NY) **121**, 456 (1979); Suppl. Progr. Theor. Phys. **64**, 436 (1978); A. Onuki and K. Yamazaki, and K. Kawasaki, Ann. Phys. (NY) **131**, 217 (1981).
[5] D. Beysens, M. Gbadamassi, and L. Boyer, Phys. Rev. Lett. **43**, 1253 (1979); D. Beysens and M. Gbadamassi, Phys. Lett. **40**, L565 (1979).
[6] C. Rangel-Nafaile, A. B. Metzner, and K. F. Wissbrun, Macromolecules **17**, 1187 (1984).
[7] F. B. Cheikh Larbi, M. F. Malone, H. H. Winter, J. L. Halary, M. H. Leviet, and L. Monnerie, Macromolecules **21**, 3544 (1988).
[8] T. Hashimoto, T. Takebe, and S. Suehiro, J. Chem. Phys. **88**, 5874 (1988).
[9] (a) T. Hashimoto, T. Takebe, and K. Fujioka, in *Dynamics and Patterns in Complex Fluids*, edited by A. Onuki and K. Kawasaki (Springer, Heidelberg, 1990), p. 86; (b) T. Takebe and T. Hashimoto, Polym. Commun. **29**, 261 (1988).
[10] T. Takebe, R. Sawaoka, and T. Hashimoto, J. Chem. Phys. **91**, 4369 (1989).
[11] E. Helfand and G. H. Fredrickson, Phys. Rev. Lett. **62**, 2468 (1989).
[12] A. Onuki, Phys. Rev. Lett. **62**, 2472 (1989); J. Phys. Soc. Jpn. **59**, 3427 (1990).
[13] T. Takebe, K. Fujioka, R. Sawaoka, and T. Hashimoto, J. Chem. Phys. **93**, 5271 (1990).
[14] A. Nakatani, H. Kim, Y. Takahashi, Y. Matsushita, A. Takano, B. J. Bauer, and C. C. Han, J. Chem. Phys. **93**, 795 (1990).
[15] T. Hashimoto and K. Fujioka, J. Phys. Soc. Jpn. **60**, 356 (1991); T. Hashimoto and T. Kume, *ibid.* **61**, 1839 (1992).
[16] X-L. Wu, D. J. Pine, and P. K. Dixon, Phys. Rev. Lett. **66**, 2408 (1991).
[17] H. Yanase, P. Moldenaers, J. Mewis, V. Abetz, J. W. van Egmond, and G. Fuller, Rheol. Acta **30**, 89 (1991).
[18] T. Hashimoto, T. Takebe, and S. Suehiro, Polym. J. **18**, 123 (1986); T. Kume, K. Asakawa, E. Moses, K. Matsuzaka, and T. Hashimoto, Acta Polym. **46**, 79 (1995).
[19] K. Fujioka, T. Takebe, and T. Hashimoto, J. Chem. Phys. **98**, 717 (1993).
[20] T. Hashimoto, T. Takebe, and K. Asakawa, Physica A **194**, 338 (1993).
[21] A. Onuki and T. Hashimoto, Macromolecules **22**, 879 (1989).
[22] P. G. de Gennes, *Scaling Concepts in Polymer Physics* (Cornell University Press, Ithaca, 1979).
[23] The peak B in the high shear-rate regime has often been observed in previous studies (Ref. 19). The minimum A and maximum B in $\mathcal{I}_{\perp,t}(\dot{\gamma})$ are attributable to the unique shear-rate dependence of $t_{\rm inc}(\dot{\gamma})$ in the system (see Figs. 5 and 7). The maximum and minimum in the shear-rate dependence of $\mathcal{I}_{\perp,i}(\dot{\gamma})$ are now clarified to reflect the same origin, although this point was left unresolved in the previous study.
[24] The cloud point temperature drop with shear $\Delta T_c(\dot{\gamma})/T_c(0)\sim\dot{\gamma}^{0.5}$ for the near-critical mixtures was interpreted as a suppression of spinodal decomposition under shear (Refs. 10,19). It is tempting to interpret the behavior for the off-critical mixtures given by Eq. (5) in terms of a suppression of nucleation and growth under shear.
[25] It should be noted that, in the case of $\Delta T(0)=10$ and 4 K, we found only the low shear regime in which $t_{\rm inc}(\dot{\gamma})$ increases with $\dot{\gamma}$. We expect that we can find the high shear regime in these cases too, in which $t_{\rm inc}(\dot{\gamma})$ decreases with $\dot{\gamma}$. However a confirmation of this point will be left for future work.
[26] T. Hashimoto, K. Matuzaka, E. Moses, and A. Onuki, Phys. Rev. Lett. **74**, 126 (1995).